

Synthesis and Spectroscopic Properties of Optical Probe Based on Schiff Base with Biological Application

Mevlüt BAYRAKCI^{1*}, Bahar YILMAZ²

ABSTRACT: A series of facile optical probe has been easily developed by a one-step Schiff base type reaction of 2,4-dihydroxybenzaldehyde and *ortho*, *meta* or *para* aminophenol. Schiff base compounds as fluorescence sensor were utilized to identify metal ions by spectrophotometric techniques. The data of absorption and emission spectra displayed the extraordinary selective and sensitive sensor properties for Schiff base probe derived from *ortho* aminophenol (**SB-2**) toward Al³⁺ ions. Upon introducing Al³⁺ ions, an excellent increase in the fluorescence intensity of the probe (**SB-2**) resulting in color change was observed because of blocking the photoinduced electron transfer (PET) mechanism of azomethine unit. The specific bonding mode of probe (**SB-2**) with Al³⁺ was verified by using a series of spectroscopic techniques such as FT-IR, ¹H NMR, and UV-vis (Job-plot data). The detection limit of probe (**SB-2**) toward Al³⁺ was determined around 10⁻⁷M. Furthermore, cell imaging studies of probe (**SB-2**) were also performed and from these experiments, it was seen that the presence of even trace amounts of Al³⁺ in living cells could be noticeably detected by (**SB-2**). In this study, antimicrobial properties of Schiff base compounds were also carried out towards some selected bacteria species. This presented work provides a method for design, facile synthesis and application of effective fluorescence probes toward Al³⁺ ions in biological systems.

Keywords: Schiff base; Aluminum; Fluorescence; Cell imagine; Anti-bacterial

¹Mevlüt BAYRAKCI (Orcid ID: 0000-0002-0416-2870), Bahar YILMAZ (Orcid ID: 0000-0002-6315-3018) Karamanoğlu Mehmetbey Üniversitesi, Mühendislik Fakültesi, Biyomühendislik Bölümü, Karaman/Türkiye

*Sorumlu Yazar/Corresponding Author: Mevlut BAYRAKCI, mevlutbayrakci@gmail.com, mbayrakci@kmu.edu.tr

Geliş tarihi / Received: 23-01-2020

Kabul tarihi / Accepted: 21-04-2020

INTRODUCTION

Aluminum is the third most abundant metal in the earth's crust and extensively used as raw material after iron in a wide range of heavy industry such as electric and electronic, information technology, cosmetic manufacturing, textile, building trade, medicine and environmental protections (Zhu et al., 2016; Lacowicz, 2002; Soni et al., 2001). Furthermore, aluminum has also an important role in biological applications system as biological transformation and enzyme-catalyzed reactions (Baxter et al., 2008). Recently, a large of medical research has been showed that using of excess amount of aluminum is harmful to human health and it causes some serious diseases such as osteoporosis, Parkinson's, osteomalacia and Alzheimer's (Walton, 2006; Altschuler, 1999; Sun et al., 2016; Gupta et al., 2012) and its level of concentration has a direct effect on human health. Therefore, the detection of aluminium is of great importance due to its potential hazard. However, the detection of aluminium ions have some complications because of the lack of spectroscopic identification, the strong hydration and poor coordination ability. Nevertheless, several analytical methods such as voltammetry, atomic-absorption spectroscopy (AAS), inductively coupled plasma emission spectrometry (ICP-AES), and potentiometric and spectrophotometric sensors have been used for low level detection of aluminum ions (Gupta et al., 2015; Shoora et al., 2015; Dillen et al., 1999). However, they have some limitations such as low selectivity, sophisticated expensive instruments, and longer period of response time in usage of these methods (Kim et al., 2012; Gupta et al., 2015). Among these techniques, the fluorescent method has most popular technique to determine the ionic species and have some advantages over other sophisticated analytical methods owing to its simplicity, low-cost analysis, high selectivity and sensitivity, naked-eye detection (Simona et al., 2016; Zhong et al., 2016). Thus, a more selective, sensitive and facile chemosensor is required to be synthesized and developed in medicinal, biological, and environmental applications with greater attention. For example, antibacterial activity is one of the most important topic in medicinal applications. In this field, Schiff base based molecules are extensively investigated with and without metal ions and some literature results reported that imine (C=N) modified molecules shows good antibacterial activities against many kinds of bacteria (Wang et al., 2011). The basic problem in the antibacterial treatment is to increase of microorganism resistance toward available drugs. Nitrofurantoin or Nifuroxazide, are example of Schiff base derivatives and these molecules are commonly applied in medicine as antibacterial agents (Sztanke et al., 2013). Although very limited literature study has been reported, some of them are still in progress. Therefore, the development of novel Schiff base type of organic compounds as a potential drug molecule is the center of some researches.

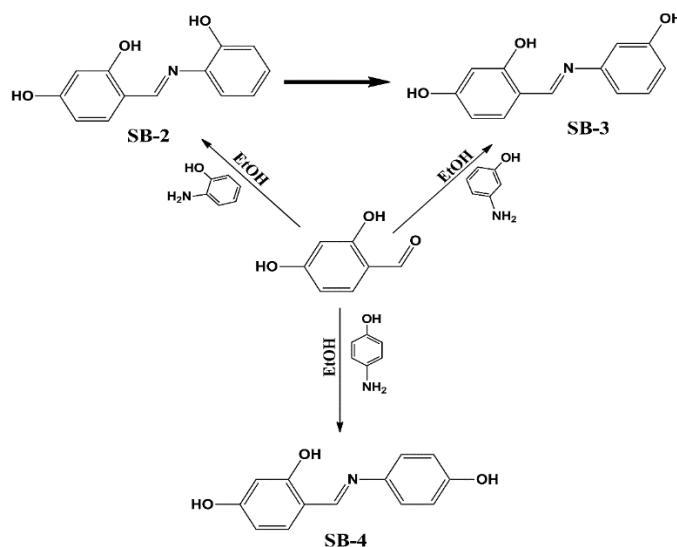
In the last decades, design and synthesis of high selective and sensitive fluorescent chemosensors have attracted great interest from current researchers due to the possible applications in different fields such as environmental, clinic and medicine (Santos-Figueroa et al., 2013; Janakipriya et al., 2016; Jeyanthi et al., 2013). To date, a limited number of chemosensor based Schiff base have been presented in literature for the detection of aluminum ions (Tian et al., 2015). The basic reason for the lesser development of aluminium chemosensors is owing to the poor coordination ability of aluminium with respect to the transition metal ions (Soroka et al., 1987). Based on this knowledge, herein, a series of Schiff base chemosensors **SB-2**, **SB-3** and **SB-4** which show an excellent selective and sensitive fluorescence enhancement response to Al^{3+} ions have been synthesized by Schiff-base condensation reaction from the corresponding *ortho*, *meta* and *para* aminophenol and 2,4-dihydroxybenzaldehyde as outlined in Scheme 1 and characterized by different spectroscopic techniques. To see the usability of these Schiff base derivatives as both potential antibacterial drug toward some selected bacteria and

potential chemosensor for aluminum imagine in living cell line, some biological experiments such as antibacterial tests based disc diffusion and cell applications were also performed.

MATERIALS AND METHODS

General

2,4-dihydroxybenzaldehyde, *ortho*, *meta* and *para* aminophenol m-phenylenediamine and all the metal salts were of analytical grade and purchased from Sigma-Aldrich or Merck and was further used without any purification. ^1H NMR spectra was generated by Agilent Premium Compact spectrometer operating at 600 MHz. Bruker Vertex FT-IR spectrometer (ATR) was used for FT-IR spectra. UV-vis absorbance spectra were collected by a Shimadzu UV-1800 and the fluorescence measurements were recorded on Hitachi F-7100. Aqueous solutions were deionized through a Millipore Milli-Q Plus water purification system.



Scheme 1. Synthetic illustration for the preparation of optical probes based Schiff base

Synthesis of Schiff bases (SB-2, SB-3 and SB-4)

Schiff bases (SB-2, SB-3 and SB-4) were synthesized by following modified literature procedure (Gupta et al., 2015; Murtaza et al., 2016). Briefly, to a stirred solution of corresponding *ortho*, *meta* or *para* aminophenol compounds (1.5 mmol) in 20 mL absolute ethanol (for **SB-2**, **SB-3** and **SB-4**, respectively) was added 1.5 mmol of 2,4-dihydroxybenzaldehyde; the reaction mixture was stirred under reflux for 18 h. After completion of the reaction, excess amount of solvent was removed under reduced pressure and the solid residue was washed with 1 N HCl, brine and excess amount of water. The crude product was crystallized from CH_2Cl_2 - $\text{C}_2\text{H}_5\text{OH}$ (1:1) solvent system (Scheme 1). **SB-2**: Dark orange solid with 77% yields, FT-IR (ATR cm^{-1}): 1625 (C=N stretching). ^1H NMR (600 MHz DMSO): δ 14.19 (bs, 1H, OH) 10.12(s, 1H, OH), 9.61 (s, 1H, OH), 8.75 (s, 1H, CH=N), 7.35 (d, J = 8.4 Hz, 1H, Ar-H), 7.27 (d, J = 7.8 Hz, 1H, Ar-H), 7.04 (m, 1H, Ar-H), 6.92 (d, J = 8.1 Hz, 1H, Ar-H), 6.83 (m, 1H, Ar-H), 6.33 (d, J = 8.4 Hz, 1H, Ar-H), 6.22 (s, 1H, Ar-H). Anal. calcd. For $\text{C}_{13}\text{H}_{11}\text{O}_3\text{N}$: C, 68.11; H, 4.84; N, 6.11. Found: C, 68.09; H, 4.90; N, 6.19%. **SB-3**: Dark yellow solid with 70% yields, FT-IR (ATR cm^{-1}): 1621 (C=N stretching). ^1H NMR (600 MHz DMSO): δ 14.18 (bs, 1H, OH) 10.12 (s, 1H, OH), 9.63 (s, 1H, OH), 8.76 (s, 1H, CH=N), 7.33 (d, J = 8.4 Hz, 1H, Ar-H), 7.25 (d, J = 7.8 Hz, 1H, Ar-H), 7.03 (m, 1H, Ar-H), 6.91 (d, J = 8.1 Hz, 1H, Ar-H), 6.84 (m, 1H, Ar-H), 6.33 (d, J = 8.4 Hz, 1H, Ar-H), 6.21 (s, 1H, Ar-H). Anal. calcd. For $\text{C}_{13}\text{H}_{11}\text{O}_3\text{N}$: C, 68.11; H, 4.84; N, 6.11. Found: C, 68.03; H, 4.80; N, 6.07%. **SB-4**: Dark yellowish solid with 73% yields, FT-IR (ATR cm^{-1}): 1619 (C=N stretching). ^1H NMR (600 MHz

DMSO): δ 14.18 (bs, 1H, OH) 10.12 (s, 1H, OH), 9.66 (s, 1H, OH), 8.77 (s, 1H, CH=N), 7.34 (d, $J=8.4$ Hz, 1H, Ar-H), 7.27 (d, $J=7.8$ Hz, 1H, Ar-H), 7.08 (t, 1H, Ar-H), 6.93 (d, $J=8.1$ Hz, 1H, Ar-H), 6.83 (m, 1H, Ar-H), 6.34 (d, $J=8.4$ Hz, 1H, Ar-H), 6.21 (s, 1H, Ar-H). Anal. calcd. For $C_{13}H_{11}O_3N$: C, 68.11; H, 4.84; N, 6.11. Found: C, 68.03; H, 4.88; N, 6.15%.

UV-vis and fluorescence studies

The stock solutions of **SB-2**, **SB-3**, and **SB-4** (1mM), the guest nitrate salts of cations (Li^+ , Na^+ , Ag^+ , Ca^{2+} , Ba^{2+} , Co^{2+} , Cs^+ , Cu^{2+} , Mg^{2+} , Hg^{2+} , Mn^{2+} , Pb^{2+} , Ni^{2+} , Sr^{2+} , Zn^{2+} and Al^{3+}) (1 mM) in DMF were prepared. In spectrophotometric experiments, the volume of studied solutions was adjusted as 2.0 mL. Titration experiments were performed by addition of corresponding amount of cation solutions to a DMF solution of **SB-2**, **SB-3**, and **SB-4**. All emission spectra were obtained at room temperature under the excitation of 400 nm. The absorption spectra of **SB-2**, **SB-3**, and **SB-4** in the presence and absence of cations were recorded in the range of 200–600 nm in a UV-Vis spectrophotometer. The solutions were scanned (1200 nm/min) with 400 watt of PMT voltage in a spectrofluorometer with the range of 430-750 nm. The widths of the slit for the both excitation and emission were adjusted at 10 nm. The fluorescence intensity at 500 nm was determined under the excitation at the wavelength of 400 nm.

Biological applications

The living MCF7 cells were provided by ATCC (American Type Culture Collection, Rockville, MD, USA). MCF7 cells were incubated with $10\mu M$ of Al^{3+} ions in the culture medium at $37^\circ C$ for 1 h and washed with phosphate buffered saline (PBS) followed by the addition of $20\mu M$ **SB-2**. Bright field and fluorescent images were taken from Leica DM3000 fluorescence microscopy (FM) (Cicekbilek et al., 2019). Antimicrobial susceptibility was tested by the disk diffusion method on LB and NB agar, according to the guidelines of the National Committee for Clinical Laboratory Standards (NCCLS) (Fiebelkorn et al., 2013). Briefly, disks containing Schiff bases **SB-2**, **SB-3**, and/or **SB-4** incubated at $37^\circ C$ for 24 h were placed on NB agar plates for gram positive bacteria *B. subtilis* or on LB agar gram negative bacteria for *E. coli*, respectively. After this time, resistance or susceptibility behaviors of *B. subtilis* or *E. coli* towards Schiff bases **SB-2**, **SB-3**, and/or **SB-4** was monitored by measuring of the obtained inhibition zone diameters at different incubation temperatures (Tahriri et al., 2017).

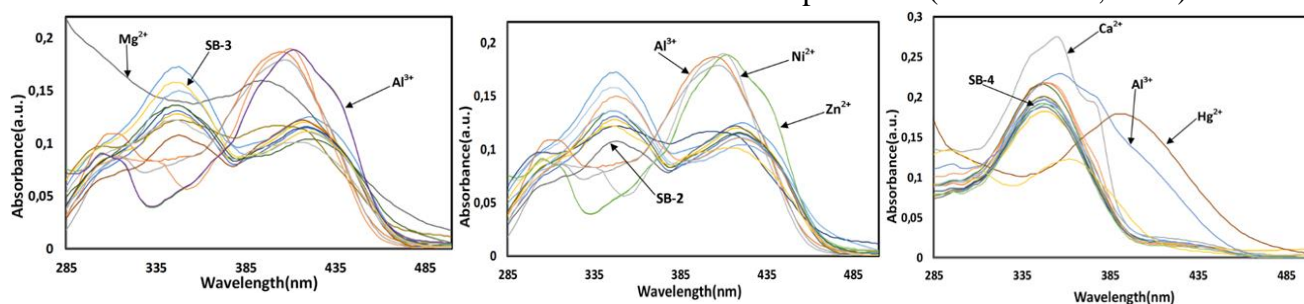


Figure 1. UV-Vis absorption spectra of compounds **SB-2**, **SB-3** and **SB-4** ($10\mu M$) in the absence and presence of different metal ions (20 equiv.) such as Li^+ , Na^+ , Ag^+ , Ca^{2+} , Ba^{2+} , Co^{2+} , Cs^+ , Cu^{2+} , Mg^{2+} , Hg^{2+} , Mn^{2+} , Pb^{2+} , Ni^{2+} , Sr^{2+} , Zn^{2+} and Al^{3+} at room temperature.

RESULTS AND DISCUSSION

UV-vis absorption analysis

The UV-vis absorption spectrum of the Schiff bases **SB-2**, **SB-3**, and **SB-4** towards various metal cations was explored in dimethylformamide (DMF) solution ($10\mu M$) in the presence of 20 equiv. of metal cations. As seen in Figure 1, the absorption spectrum of **SB-2**, and **SB-3**, exhibited two broad absorption bands at around 348 nm and 414 nm attributable to $\pi-\pi^*$ transition of the imine moiety. The

small changes for the position of absorption bands was observed after the addition of Al^{3+} , Ni^{2+} and Zn^{2+} owing to the imine nitrogen ($\text{CH}=\text{N}$) was involved in coordination with metal ion. However, considerable changes in the absorption spectra of the **SB-2**, and **SB-3** were not observed over other metal ions. Similar changes in the spectra of **SB-4** were observed for the Hg^{2+} , Ca^{2+} and Al^{3+} . Considering these changes, powerful hyperchromic changes was only seen for **SB-2**, and **SB-3** at around 348 nm and 414 nm with Al^{3+} ions.

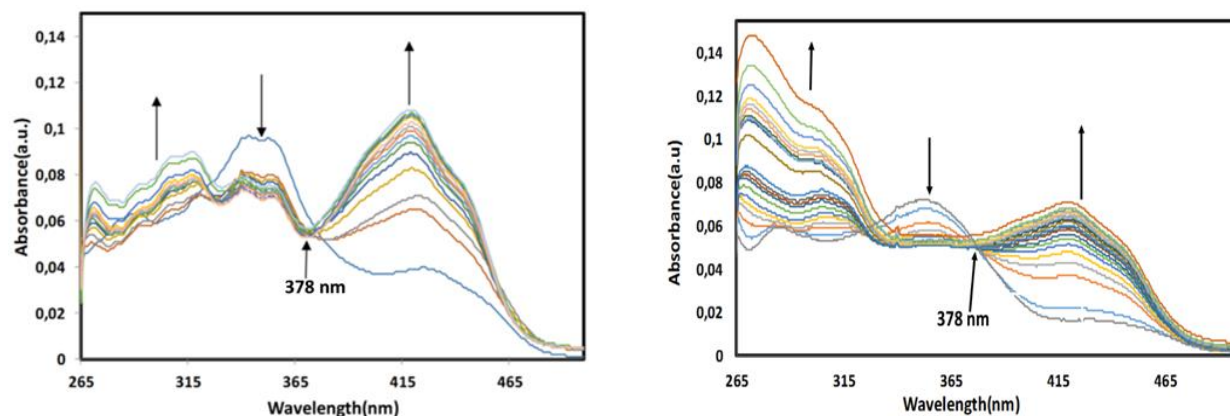


Figure 2. UV-Vis absorption spectra of compounds **SB-2** and **SB-3** ($10\mu\text{M}$), respectively, upon the titration of Al^{3+} (from 0 to 2 equiv.) at room temperature.

The binding properties of **SB-2** and **SB-3** with Al^{3+} ions were studied by UV-vis titration in DMF solution (Figure 2). Upon addition of increasing amounts of Al^{3+} (0.0 to 2.0 equiv.), absorption bands of **SB-2** appeared at 272 nm and 420 nm was gradually enhanced with increasing concentration of Al^{3+} , while the intensities of absorption at 350 nm were decreased. During the titration of **SB-2** with Al^{3+} , the clear isobestic point were observed at 378 nm which means that an equilibrium and interaction generated between **SB-2** and Al^{3+} . These observations supported the definite conversion of **SB-2** to the corresponding aluminum metal complex having a precise stoichiometric ratio between **SB-2** and Al^{3+} formed in solution. Subsequently, the further addition of Al^{3+} did not change the UV-vis spectra of **SB-2**. The titration configuration of **SB-2** with Al^{3+} shown indicated 1 equiv. of Al^{3+} reacting with same equiv. of **SB-2** could quickly reached an equilibrium, showing complex formation between **SB-2** and Al^{3+} with 1:1 stoichiometry. Furthermore, same results were also observed for complex structure of **SB-3** with Al^{3+} . Fluorescence emission studies was performed for getting and interpreting the more accurate and precise spectrophotometric results since absorption spectroscopy was complementary part of emission spectroscopy.

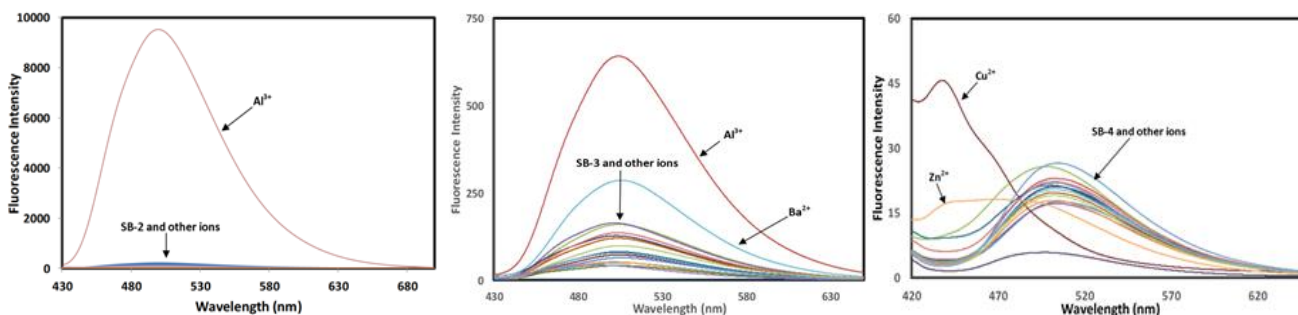


Figure 4. Fluorescence emission spectra (at 500 nm) of compounds **SB-2**, **SB-3** and **SB-4** ($10\mu\text{M}$) in DMF in the presence of different metal ions (20 equiv.) such Li^+ , Na^+ , Ag^+ , Ca^{2+} , Ba^{2+} , Co^{2+} , Cs^+ , Cu^{2+} , Mg^{2+} , Hg^{2+} , Mn^{2+} , Pb^{2+} , Ni^{2+} , Sr^{2+} , Zn^{2+} and Al^{3+} . ($\lambda_{\text{ex}} = 400\text{ nm}$).

Fluorescence emission analysis

High selectivity is necessary to define the excellent chemosensor. Therefore, to evidence the usability of the synthesized Schiff bases **SB-2**, **SB-3**, and **SB-4** as a selective sensor, the fluorescence behavior of **SB-2**, **SB-3**, and **SB-4** was investigated by using Hitachi F-7100 Spectrofluorometer upon the addition of selected metal ions such as Li^+ , Na^+ , Ag^+ , Ca^{2+} , Ba^{2+} , Co^{2+} , Cs^+ , Cu^{2+} , Mg^{2+} , Hg^{2+} , Mn^{2+} , Pb^{2+} , Ni^{2+} , Sr^{2+} , Zn^{2+} and Al^{3+} . Schiff base **SB-2**, **SB-3**, and **SB-4** did not show any considerable emission band alone at 500 nm when the excitation wavelength was at 400 nm. After addition of metal ions such as Li^+ , Na^+ , Ag^+ , Ca^{2+} , Ba^{2+} , Co^{2+} , Cs^+ , Cu^{2+} , Mg^{2+} , Hg^{2+} , Mn^{2+} , Pb^{2+} , Ni^{2+} , Sr^{2+} and Zn^{2+} (Figure 4), Schiff base **SB-2**, **SB-3**, and **SB-4** did not still demonstrate any significant fluorescent response. However, upon addition of Al^{3+} ions, only Schiff base **SB-2** and **SB-3** exhibited excellent response with more than 335-fold and 11-fold fluorescent enhancement. This fascinating increase in fluorescence intensity of **SB-2** demonstrated that selective and excellent ‘off-on’ type fluorescent sensor behavior of **SB-2** had occurred toward Al^{3+} .

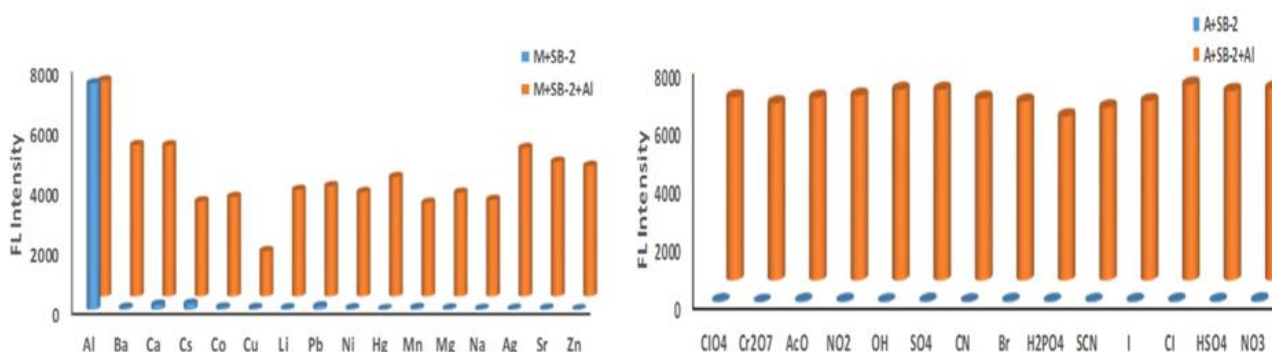


Figure 5. Fluorescence intensity of **SB-2** and its complexation with Al^{3+} in the presence of various cations or anions. ($\lambda_{\text{exc}} = 400 \text{ nm}$).

For the investigation of the selectivity performance of **SB-2** or **SB-3** toward Al^{3+} ions, some competing experiments were carried out by using metal ions. Interferences of metal cations were investigated by treating **SB-2** or **SB-3** with 20 equiv. of Al^{3+} in the presence of equal to competing metal cations (Li^+ , Na^+ , Ag^+ , Ca^{2+} , Ba^{2+} , Co^{2+} , Cs^+ , Cu^{2+} , Mg^{2+} , Hg^{2+} , Mn^{2+} , Pb^{2+} , Ni^{2+} , Sr^{2+} and Zn^{2+}). As shown in Figure 5, it was observed that fluorescence response of compounds **SB-2** or **SB-3** for Al^{3+} was not affected by addition of competing metal ions or some selected anions considerably. But the relatively reducing of the fluorescent responses for complex structure of **SB-2- Al^{3+}** or **SB-3- Al^{3+}** upon addition of some studied metal ions was also observed. Despite addition of these metal ions, it was seen that fluorescence responses of **SB-2** and **SB-3** toward Al^{3+} ions could be easily and clearly detectable under UV-light by naked-eye. Both **SB-2** and **SB-3** still have an efficient ‘turn-on’ rate for the detection of Al^{3+} . From the competition results, it was seen that Schiff bases **SB-2** and **SB-3** as a probe had high selectivity and specificity toward Al^{3+} over other ions such as Li^+ , Na^+ , Ag^+ , Ca^{2+} , Ba^{2+} , Co^{2+} , Cs^+ , Cu^{2+} , Mg^{2+} , Hg^{2+} , Mn^{2+} , Pb^{2+} , Ni^{2+} , Sr^{2+} , and Zn^{2+} . Among **SB-2** solutions with and without metal cations excited at 400 nm, only the **SB-2** solutions mixed with Al^{3+} ions showed an extraordinary color change from toneless to brilliant fluorescent blue and this change was easily detected by the naked eye under UV light (Figure 6).

The observed fluorescence enhancement can be explained by the blocking the photoinduced electron transfer (PET) process when **SB-2** is bound with Al^{3+} (Ding et al., 2015). The lone pair electrons of azomethine ($\text{CH}=\text{N}$) unit of probe **SB-2** delocalize (un-blocking of PET) to the two phenyl rings in the Schiff base structure and quenches the fluorescence intensity. After addition of Al^{3+} , this lone pair electron of imine group is perturbed by the coordination of Al^{3+} and this interaction give rise to an

increase in fluorescence intensity. This situation proposes that the photo induced electron transfer (PET) is the favorable mechanism to explain “off-on” type of fluorescence for **SB-2** after binding to Al^{3+} .

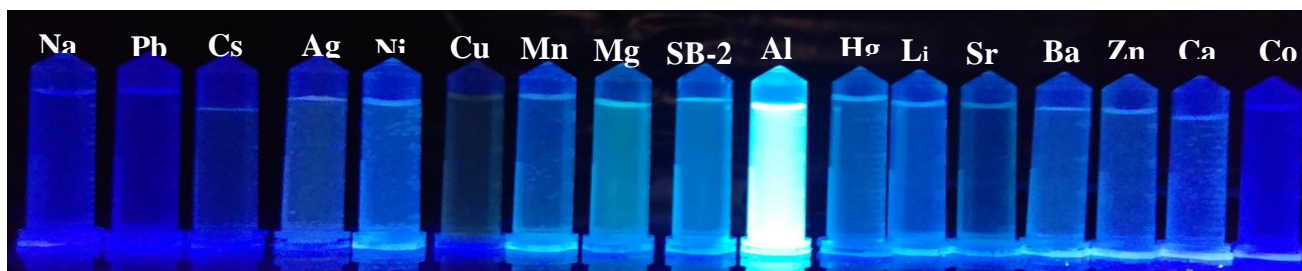


Figure 6. Images showing the corresponding fluorescence color changes of **SB-2** with and without metal cations (20 equiv.) under UV light.

To further examine the sensing properties of **SB-2** and **SB-3**, sensitivity of **SB-2** and **SB-3** as a probe toward Al^{3+} ions was investigated by the fluorescence titration experiments by increasing concentration of Al^{3+} ions (0-20 equiv.) at 500 nm (Figure 7) and the detection limit of Al^{3+} was estimated based on the fluorescence titration profile. The detection limit of **SB-2** in recognizing Al^{3+} was found to be $6.45 \cdot 10^{-7} \text{M}$ which was lower than some presented Al^{3+} selective chemosensors (Ding et al., 2015, Tian et al., 2015; Zhou et al., 2015). This result has shown that this sensor could be used for both detection and monitoring of sub-micromolar concentration of aluminum ions in biological and environmental systems.

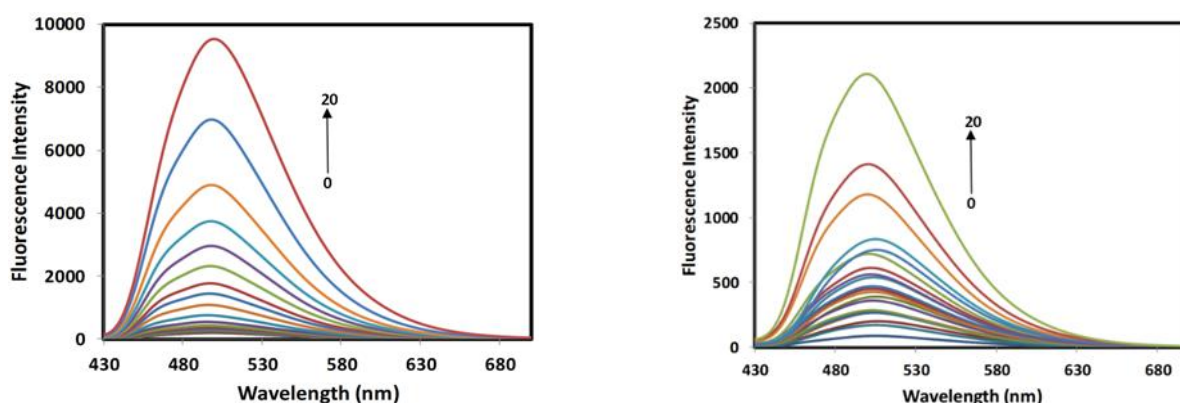


Figure 7. Fluorescence titration spectra of **SB-2** and **SB-3**, respectively, upon addition of Al^{3+} (from 0 to 20 equiv.) with an excitation of 400 nm, and an emission of 500 nm.

The molar ratio of the coordination between **SB-2** and Al^{3+} was studied by the Job's plot method (Job, 1928) as shown in Figure 8. In this method, each experiment carried out with different concentrations of **SB-2** and Al^{3+} ions with maintaining the total concentration at 20 μM . The plot obtained by measuring the fluorescence intensity at 500 nm for nine experiments with molar fraction of **SB-2** (0.1 to 0.9). The maximum fluorescence intensity at 500 nm was observed when the molar fraction was 0.5. This data showed that 1 mole of **SB-2** probe and Al^{3+} participated in the complex formation and binding mode was determined as 1:1 stoichiometry. Furthermore, the binding constant of the probe **SB-2** with Al^{3+} were calculated by the Benesi–Hildebrand method (Benesi and Hildebrand, 1949). From curve fitting of fluorescence intensity of probe **SB-2** against the reciprocal of the Al^{3+} concentration, this plot yielded a linear fit as seen in Figure 9. The value of the binding constant was calculated as $2.8 \cdot 10^5 \text{M}^{-1}$ for probe **SB-2** from this equation. In addition, the linear plot also proved the 1:1 complexation

behavior of **SB-2** to Al^{3+} . Because, if a 1:1 metal-probe complex is formed between receptor and metal ions, Benesi-Hildebrand plot should be linear (Benesi and Hildebrand, 1949).

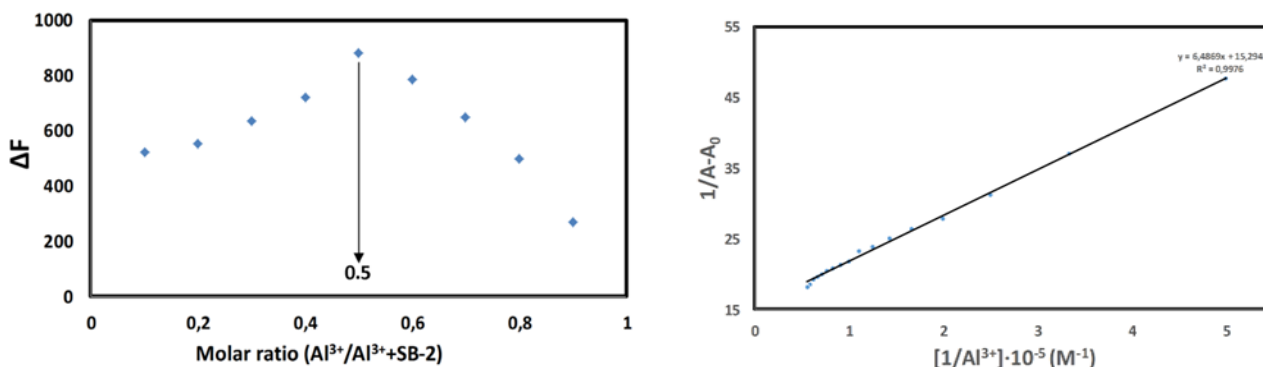


Figure 8. Job's plot and Benesi-Hildebrand plot for determining the complexation behavior of **SB-2** to Al^{3+} in DMF.

In related to stoichiometry, the binding site participated in complexation was clarified by FT-IR and ^1H NMR titration experiments along with stoichiometry confirmation as presented in Figure 9 and 10. The IR spectra of **SB-2** and **SB-2- Al^{3+}** showed that the characteristics frequencies of **SB-2** with different stoichiometric ratio of Al^{3+} exhibited significant changes as compared with those of the **SB-2** without Al^{3+} . The IR spectra of the free **SB-2** showed the absence of bands at around 1735 and 3300 cm^{-1} attributable to the carbonyl $\nu(\text{C}=\text{O})$ and $\nu(\text{NH}_2)$ stretching vibrations and a clear strong new band at around 1625 cm^{-1} due to azomethine $\nu(\text{HC}=\text{N})$ linkage. All these existing and disappearing signals in FT-IR indicated that amino and aldehyde groups in starting reactants (Scheme 1) were converted into the **SB-2** and synthesis of the **SB-2** was successfully carried out. The comparison of FT-IR spectra of free **SB-2** and its Al^{3+} complex (Figure 2) demonstrated that **SB-2** probe was principally coordinated to the Al^{3+} ion. The strong band appearing at around 1625 cm^{-1} due to azomethine group shifted to a lower frequency at 1589 cm^{-1} in Al^{3+} complex, indicating participation of azomethine group in the complexation with the Al^{3+} ion.

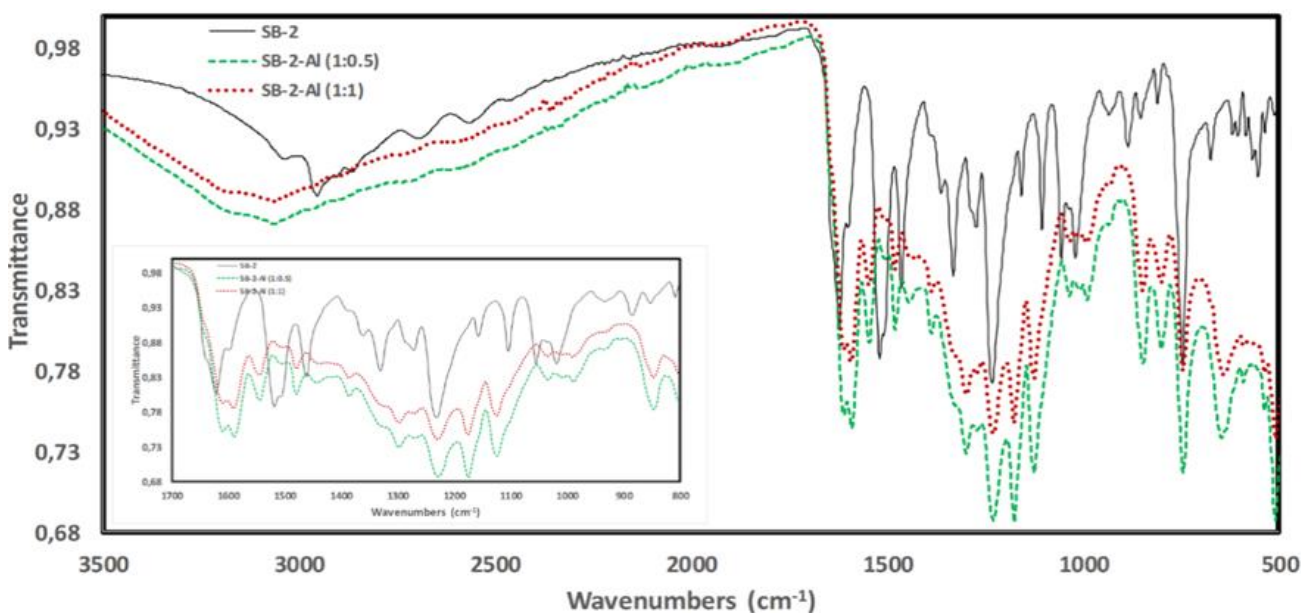


Figure 9. The FT-IR spectra data of **SB-2** in presence of different amount of Al^{3+} .

To better understand the complexation between the probe **SB-2** and Al^{3+} , ^1H NMR titration experiments of **SB-2** in $\text{DMSO-}d_6$ were examined by addition of varied equiv. of Al^{3+} . As seen in Figure 10, three phenolic -OH signals belonging to **SB-2** were observed at around 9.61, 10.12 and 14.19 ppm which showed that it was very acidic due to the intramolecular hydrogen bonding (Figure 11). While the phenolic OH proton at 14.19 ppm disappeared when added of 0.5 and 1.0 equiv. of Al^{3+} to **SB-2** solution, the other signal at around 10.12 and 9.61 ppm shifted to downfield (Keskin and Bayrakci, 2019). Also, the imine (CH=N) proton of **SB-2** at 8.76 ppm was slightly shifted downfield. This shift for the imine proton was probably due to de-shielding of the azomethine group after coordination of **SB-2** with Al^{3+} . All these shifting and/or disappearing of signals showed that both phenolic OH group located in *ortho* position and imine group of **SB-2** were efficient on complex formation between **SB-2** and Al^{3+} .

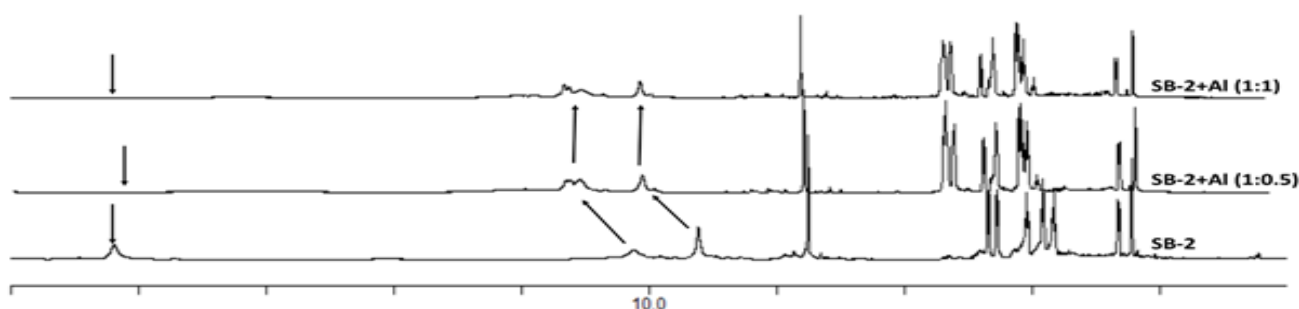


Figure 10. ^1H NMR spectra of **SB-2** in $\text{DMSO-}d_6$ at 25 °C and the corresponding changes after the addition of aluminum nitrate.

Biological Applications

SB-2 was successfully applied for imaging of Al^{3+} ions in human breast cancer cells, MCF7 under fluorescence microscope. Cells treated with **SB-2**, without any Al^{3+} and treated with Al^{3+} were used as controls. When MCF7 cells were incubated with **SB-2** (20 μM), it was not seen any fluorescence response. However, after addition of Al^{3+} ions, a brilliant red fluorescence was sighted in the MCF7 cells (Figure 11). Merged images of fluorescence and bright-field showed that fluorescence signals were detected in the intra-cellular zone (Kim et al., 2007), showing the distribution of Al^{3+} and cell membrane permeabilities of **SB-2** molecules. On the other hand, Figure 12 indicated that **SB-2** could stain Al^{3+} ions in living cells without any harm (cells remain alive even after several hours of exposure to 20 μM **SB-2**), making it useful to monitor Al^{3+} in biological systems.

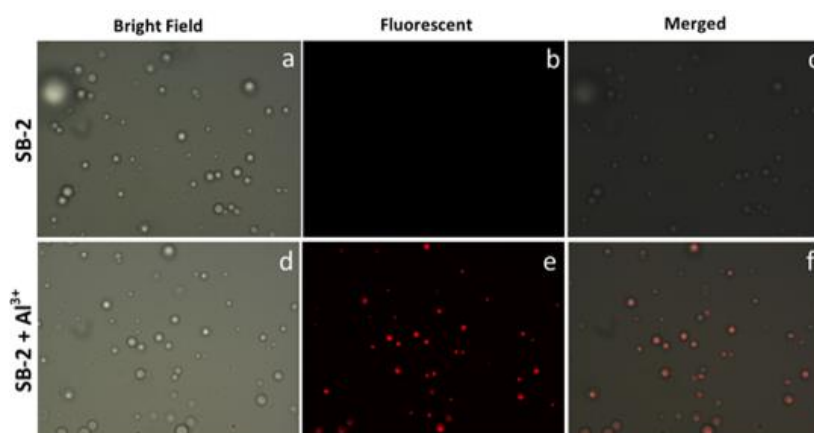


Figure 11. Fluorescence images of Al^{3+} using probe **SB-2** in MCF7 cells: (a) bright field image of MCF7 cells treated with probe **SB-2**; (b) fluorescence image of MCF7 cells with probe **SB-2**; (c) merged image of (a) and (b); (d) bright field image of MCF7 cells treated with probe **SB-2** and Al^{3+} ; (e) fluorescence image of MCF7 cells treated with probe **SB-2** and Al^{3+} ; (f) merged image of (d) and (e).

To further demonstrate the practical biological application of **SB-2** and other Schiff bases **SB-3** and **SB-4**, antimicrobial properties of them towards human pathogenic gram positive and gram-negative bacteria were evaluated by measuring the zone of inhibition in disc diffusion method. In Figure 12, measured zones of inhibition for the Schiff bases ranged from 2.0 to 2.2 cm for **SB-2**, and **SB-3**, and 1.9 to 2.0 cm for **SB-4** against gram positive bacteria *B. subtilis*. In addition, the zones of inhibition for the Schiff bases ranged from 2.0 to 2.1 cm for **SB-2**, 2.0 to 2.2 cm for **SB-3**, and 2.1 to 2.3 cm for **SB-4** toward gram negative bacteria *E. coli*. Based on zones of inhibition results, Schiff base based compounds **SB-2**, **SB-3** and **SB-4** showed better activity against both gram positive and gram-negative bacteria lines. Obtained antimicrobial data for **SB-2**, **SB-3** and **SB-4** is not surprising. Because, it is well-known that the azomethine linkage (-C=N-) in the Schiff base structure indicates widespread biological activities due to increased lipo-solubility of the Schiff base molecules in crossing cell membrane of the microorganism by blocking the protein synthesis which inhibits further growth of the organisms (Neelakantan et al., 2008).

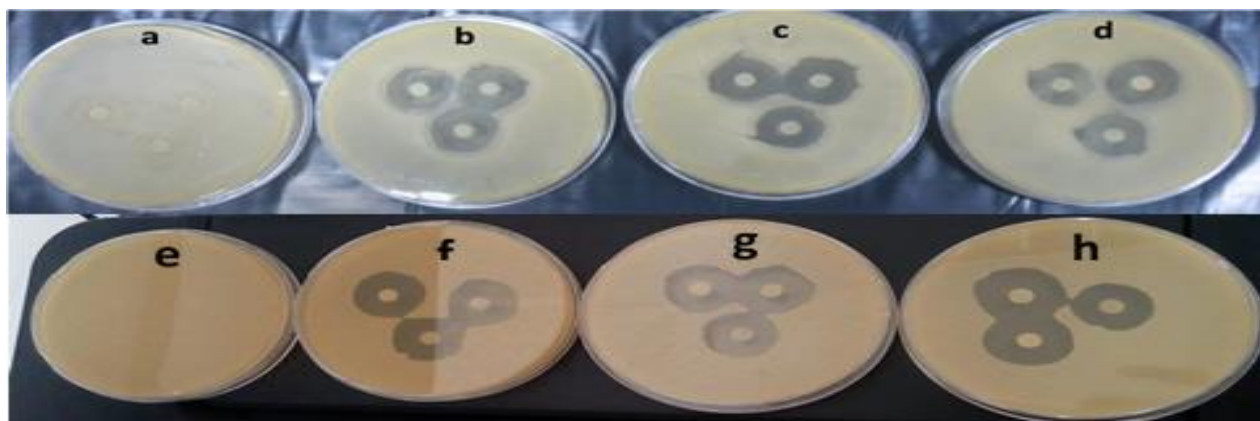


Figure 12. Photograph of antibacterial test of the Schiff bases **SB-2**, **SB-3** and **SB-4** after 24 h of incubation at 37 °C: (a) control and *E. coli*; (b) **SB-2** and *E. coli*; (c) **SB-3** and *E. coli*; (d) **SB-4** and *E. coli*; (e) control and *B. subtilis*; (f) **SB-2** and *B. subtilis*; (g) **SB-3** and *B. subtilis*; and (h) **SB-4** and *B. subtilis*.

CONCLUSION

In conclusion, detection of Al^{3+} ions with highly selective and sensitive by a very simple and low-cost fluorescence sensor (**SB-2**) were presented successfully. **SB-2** showed high sensitivity with the detection limit at around $6.45 \cdot 10^{-7}$ M in the micromolar scale. The predicted configuration of the (**SB-2**)– Al^{3+} complex formation was well-characterized to be 1:1 by spectroscopic analyses. Beyond that, (**SB-2**) was utilized to detect sensitively the Al^{3+} ions in living cells by emitting visible fluorescence. Cell applications indicated that (**SB-2**) could be used as an excellent fluorescence probe for visualizing of Al^{3+} ions in cell lines. Furthermore, antibacterial properties of Schiff bases **SB-2**, **SB-3** and **SB-4** were also explored by disc diffusion method.

REFERENCES

- Altschuler E, 1999. Aluminum-containing antacids as a cause of idiopathic Parkinson's disease. *MedicalHypotheses* 53(1):22-23.
- Baxter NJ, Blackburn GM, Marston JP, Hounslow AM, Cliff MJ, Bermel W, Williams NH, Hollfelder F, Wemmer DE, Waltho JP, 2008. Anionic charge is prioritized over geometry in aluminum and magnesium fluoride transition state analogs of phosphoryl transfer enzymes. *Journal of American Chemical Society* 130: 3952-3958.

- Benesi HA, Hildebrand JH, 1949. A spectrophotometric investigation of the interaction of iodine with aromatic hydrocarbons. *Journal of American Chemical Society* 71(8):2703–2707.
- Cicekbilek F., Yilmaz B., Bayrakci M., Gezici O, 2019. An Application of a Schiff-Base Type Reaction in the Synthesis of a New Rhodamine-Based Hg(II)-Sensing Agent. *Journal of Fluorescence* 29:1349–1358.
- Dilleen JW, Birch BJ, Haggett BGD, 1999. Electrochemical detection of aluminium using single-use sensors. *Analytical Communications* 36:363-365.
- Ding WH, Wang D, Zheng XJ, Ding WJ, Zheng JQ, Mu WH, Cao W, Jin LP, 2015. A turn-on fluorescence chemosensor for Al³⁺, F⁻ and CN⁻ ions, and its application in cell imaging. *Sensors and Actuators B: Chemical* 209:359-367.
- Fiebelkorn KR, Crawford SA, McElmeel ML, Jorgensen JH, 2003. Practical disk diffusion method for detection of inducible clindamycin resistance in *Staphylococcus aureus* and coagulase-negative staphylococci. *Journal of Clinical Microbiology* 41(10):4740-4744.
- Gupta VK, Ganjali MR, Norouzi P, Khani H, Nayak A, Agarwal S, 2011. Electro-chemical analysis of some toxic metals by ion selective electrodes. *Critical Reviews in Analytical Chemistry* 41(4):282–313.
- Gupta VK, Shoorra SK, Kumawat LK, Jain AK, 2015. A highly selective colorimetric and turn-on fluorescent chemosensor based on 1-(2-pyridylazo)-2-naphthol for the detection of aluminium(III) ions. *Sensors and Actuators B: Chemicals* 209:15–24.
- Gupta VK, Mergu N, Kumawat LK, Singh AK, 2015. A reversible fluorescence “off–on–off” sensor for sequential detection of aluminum and acetate/fluoride ions. *Talanta* 144(1):80-89.
- Gupta SD., Revathi B., Mazaira GI., Galigniana MD., Subrahmanyam CVS., Gowrishankar NL., Raghavendra NM, 2015. 2,4-dihydroxy benzaldehyde derived Schiff bases as small molecule Hsp90 inhibitors: Rational identification of a new anticancer lead. *Bioorganic Chemistry* 59: 97-105.
- Janakipriya S, Cheretty NR, Korrapati P, Thennarasu S, Mandal AB, 2016. Selective interactions of trivalent cations Fe³⁺, Al³⁺ and Cr³⁺ turn on fluorescence in a naphthalimide based single molecular probe. *Spectrochimica Acta Part A Molecular and Biomolecular Spectroscopy* 153:465–470.
- Jeyanthi D, Iniya M, Krishnaveni K, Chellappa D, 2013. A ratiometric fluorescent sensor for selective recognition of Al³⁺ ions based on a simple benzimidazole platform, *RSC Advances* 3:20984–20989.
- Job P, 1928. Formation and stability of inorganic complexes in solution. *Annales de Chimie* 9:113–203.
- Keskin S, Bayrakci M, 2019. A simple and highly sensitive turn-on Schiff base type naked-eye fluorescent sensor for aluminum ion in living cells. *Acta Chimica Slovenica* 66(4):792–801.
- Kim HM, Jung C, Kim BR, Jung SY, Hong JH, Ko YG, Lee KJ, Cho BR, 2007. Environment-sensitive two-photon probe for intracellular free magnesium ions in live tissue. *Angewandte Chemie* 46:3460–3463.
- Kim S, Noh JY, Kim KY, Kim JH, Kang HK, Nam SW, Kim SH, Park S, Kim C, Kim J, 2012. Salicylimine-based fluorescent chemosensor for aluminum ions and application to bioimaging. *Journal of Inorganic Chemistry* 51(6):3597–3602.
- Lakowicz JR, 2002. *Topics in fluorescence spectroscopy: probe design and chemical sensing*; Kluwer Academic Publishers: New York, 4-11p.
- Murtaza S., Abbas A., Iftikhar K., Shamim S., Akhtar MS., Razzaq Z., Naseem K., Elgorban AM, 2016. Synthesis, biological activities and docking studies of novel 2,4-dihydroxybenzaldehyde based Schiff base. *Medicinal Chemistry Research* 25: 2860–2871.
- Neelakantan MA, Rusalraj F, Dharmaraja J, Johnsonraja S, Jeyakumar T, Sankarayana PM, 2008. Spectral characterization, cyclic voltammetry, morphology, biological activities and DNA cleaving studies of amino acid Schiff base metal(II) complexes. *Spectrochimica Acta Part A Molecular and Biomolecular Spectroscopy*, 71(4):1599-1609.
- Santos-Figueroa LE, Moragues ME, Climent E, Agostini A, Martinez-Manez R, Sancenon F, 2013. Chromogenic and fluorogenic chemosensors and reagents for anions A comprehensive review of the years 2010–2011. *Chemical Society Review* 42(8):3489–3613.
- Shoorra SK, Jain AK, Gupta VK, 2015. A simple Schiff base based novel optical probe for aluminium (III) ions. *Sensors and Actuators B: Chemicals* 216:86–104.

- Simona T, Shellaiahb M, Srinivasadesikanc V, Lina CC, Koa FH, Sunb KW, Linc MC, 2016. A simple pyrene based AIEE active schiff base probe for selective naked eye and fluorescence off–on detection of trivalent cations with live cell application. *Sens. Actuators B* 231:18-29.
- Soni MG, White SM, Flamm WG, Regul GAB, 2001. Safety evaluation of dietary aluminum. *Regulatory Toxicology and Pharmacology* 33(1):66-79.
- Soroka K, Vithanage RS, Phillips DA, Walker B, Dasgupta PK, 1987. Fluorescence properties of metal complexes of 8-hydroxyquinoline-5-sulfonic acid and chromatographic applications. *Analytical Chemistry* 59(4):629–636.
- Sun X, Liu J, Zhuang C, Yang X, Han Y, Shao B, Song M, Li Y, Zhu Y, 2016. Aluminum trichloride induces bone impairment through TGF- β 1/Smad signaling pathway. *Toxicology* 14:49-57.
- Sztanke K, Maziarka A, Osinka A, Sztanke M 2013. An insight into synthetic Schiff bases revealing antiproliferative activities in vitro. *Bioorganic and Medicinal Chemistry* 21:3648–3666.
- Mozhgan T., Mohammad Y., Kheirollah M., Masoumeh T., Mahmood D.A, 2017. Synthesis, Characterization and Antimicrobial Activity of Two Novel Sulfonamide Schiff Base Compounds. *Pharmaceutical Chemistry Journal* 51:425–428.
- Tian J, Yan X, Yang H, Tian F, 2015. A novel turn-on Schiff-base fluorescent sensor for aluminum(III) ions in living cells. *RSC Advances* 5:107012-107019.
- Zhong Z, Zhang D, Li D, Zheng G, Tian Z, 2016. Turn-on fluorescence sensor based on naphthalene anhydride for Hg²⁺. *Tetrahedron* 72(49):8050-8074.
- Zhou D, Sun C, Chen C, Cui X, Li X, 2015. Research of a highly selective fluorescent chemosensor for aluminum(III) ions based on photoinduced electron transfer. *Journal of Molecular Structures* 1079:315-320.
- ZhuJ, Zhang Y, Wang L, Sun T, Wang M, Wang Y, Ma D, Yang Q, Tang Y, 2016. A simple turn-on Schiff base fluorescence sensor for aluminum ion *Tetrahedron Letters* 57: 3535–3539.
- Walton JR, 2006. Aluminum in hippocampal neurons from humans with Alzheimer's disease. *Neurotoxicology* 27:385-394.
- Wang JT, Wang HD 2011. Preparation of soluble p-aminobenzoyl chitosan ester by Schiff's base and Antibacterial activity of the derivatives. *International Journal of Biological Macromolecules* 48:523–529.